NUMERICAL MODELLING OF VORTICES DEVELOPMENT IN TAPERED DUCT

Grzegorz L. Pankanin, Jerzy Berlinski, Ryszard Chmielewski, Institute of Electronic Systems, Warsaw University of Technology, Warsaw, Poland

Index terms

n - *flow velocity upstream the bluff body*
n_{pc} - *flow velocity 'driving' the vortex*
w - *vortex rotation*
x - *current vortex displacement from the bluff body axis*
x_s - *length of intensive development zone*
x_k - *length of intensive development and stabilization zones*
d - *bluff body diameter*
D - *width of the duct*
r - *radius of the vortex*
Dz - *thickness of the layer*
F - *interaction force between the adjacent layers*
A - *surface area between adjacent layers*
r - *fluid density*
m - *mass*
h - *dynamic viscosity*
J - *moment of inertia*
E_{rot} - *rotation energy of layer*
E_{tot} - *total rotation energy*
k - *layer number*
t - *flow turbulence*
x,y - *co-ordinates*

Keywords: vortex meter, Karman vortex street, numerical modelling

1. Introduction

The work refers to the vortex flow meter optimisation. Searching of the optimal geometry of the meter became the fundamental task for designers. For many years their attention has been focused mainly on the bluff body as well as on the sensor designing. Numerous experiments made by authors of the paper confirm that not only the bluff body shape but also geometry of the duct impacts the vortices development. Duct walls stabilize the vortex shedding and its development process. Hence the conception of flow duct tapering in the vortices development zone. On the basis of the numerical simulation it is concluded that due to the pipe cross-section contraction (causing the flow velocity increase) the vortex rotation energy enhancement as well as vortex life-time increase has been attained.

2. Numerical modelling of the vortex development

The earlier worked out numerical model [1] is based on observation of vortex Karman street phenomenon (hot-wire anemometer and flow visualisation). The most important remarks are:

- vortices originate alternatively on both sides of the bluff body and roll downstream,
- diameter of each vortex increases with its displacement,
- traces of vortices cover a limited area,
- downstream the bluff body a „low motion" area is distinguished,
- vortices take places subsequently creating Karman street with their alternative rotation respectively,
- outside the Karman street area the flow is undisturbed.

On the basis on enumerated above remarks, the two-dimensional simple model of Karman vortex street has been considered. As it is shown in Fig.1., the circular cylinder as the bluff body is appointed in the duct limited by the walls.
According to the hot-wire as well as the flow visualisation results, the area downstream the bluff body where the vortices exists, has been divided into three zones. They considerably differ each other and in mathematical description can be treated separately.

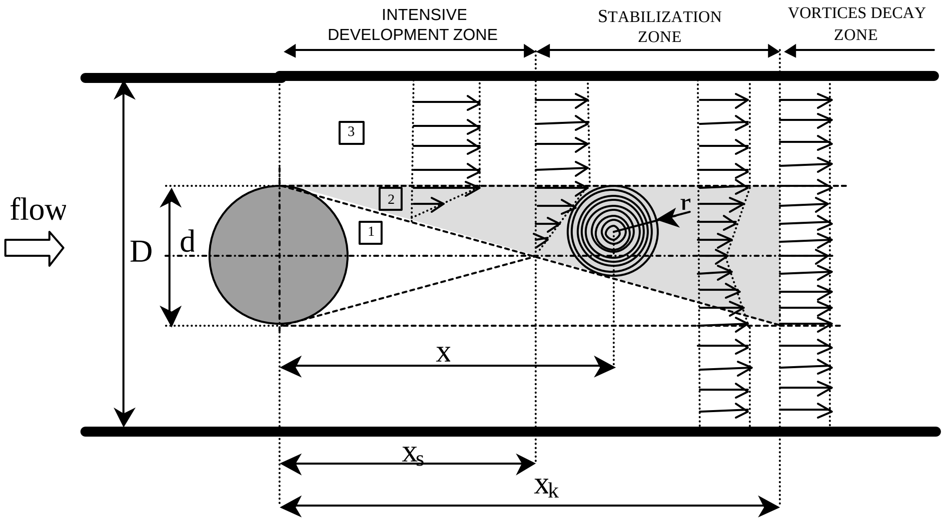

Fig.1. Vortex development behind bluff body in duct with steady cross-section
(1 - stagnation region, 2 - region of steady velocity profile, 3 - region of vortices development)

In **the intensive development zone** the vortex rolls on the boarder between the intensive development region and stagnation region. On the opposite side, the vortex is driven by the fluid stream with velocity of the region of steady velocity profile where the velocity magnitude varies with the distance **x**. The velocity "driving" the vortex is expressed by eq.(1)

$$\mathbf{v}_{pc} = \frac{\mathbf{v}}{\mathbf{2}} \cdot \frac{\mathbf{D}}{\mathbf{D} - \mathbf{d} + \frac{\mathbf{d}}{\mathbf{2}} \cdot \frac{\mathbf{x}}{\mathbf{x}_s}} \qquad \textbf{(1)}$$

The radius of the developing vortex increases with time and distance **x**, due to adding of succeeding layers:

$$\mathbf{r(x)} = \frac{\mathbf{d}}{\mathbf{4}} \cdot \frac{\mathbf{x}}{\mathbf{x}_s} \qquad \textbf{(2)}$$

Hence the rotation of the currently added layer:

$$w = \frac{\mathbf{v} \cdot \mathbf{D} \cdot \mathbf{x}_s}{\pi \cdot \mathbf{d} \cdot \mathbf{x} \cdot \left(\mathbf{D} - \mathbf{d} + \frac{\mathbf{d}}{\mathbf{2}} \cdot \frac{\mathbf{x}}{\mathbf{x}_s}\right)} \qquad \textbf{(3)}$$

It is necessary to notice that even if the rotation magnitude of each consecutive vortex layer is lower than the previous one, the rotation energy of the vortex rapidly increases along with the distance from its origin. It results from the fact, that every subsequent layer consist greater mass, so their moment of inertia rapidly increases and vortex accumulated energy grows intensively.

In **the stabilization zone** further vortex development is found, although increase of the rotation energy along with the vortex displacement is not so rapid.

The velocity "driving" the added layer is expressed by:

$$\mathbf{v}_{pc}\mathbf{(x)} = \frac{\mathbf{v}}{\mathbf{2}} \cdot \frac{(\mathbf{2x}_s - \mathbf{x}) \cdot (\mathbf{x}_k - \mathbf{x})}{(\mathbf{x}_k - \mathbf{x}_s) \cdot (\mathbf{1} - \mathbf{d}/\mathbf{2D}) \cdot \mathbf{x}_s} \qquad \textbf{(4)}$$

and rotation of the currently added layer:

$$w = \frac{\mathbf{v} \cdot \mathbf{x}_s}{\pi \cdot \mathbf{d} \cdot \mathbf{x}} \cdot \frac{(\mathbf{2x}_s - \mathbf{x}) \cdot (\mathbf{x}_k - \mathbf{x})}{(\mathbf{x}_k - \mathbf{x}_s) \cdot (\mathbf{1} - \mathbf{d}/\mathbf{2D}) \cdot \mathbf{x}_s} \qquad \textbf{(5)}$$

Finally, in **the vortices decay zone**, further layers are attached to the vortex, but they are not driven by the stream yet. Due to viscosity forces, they can be driven by the internal layers only dissipating their energy until disappearance of the vortex.

3. Conception of duct tapering

As it is well-known, the vortex meter application is limited to the range of Reynolds numbers above 10.000. Below this value the nonlinearity of the characteristic curve occurs, and at very low flow velocities the vortex shedding phenomenon is not observed at all. At very low flow velocities the vortices are unstable having little energy.
Hence the conception of the duct modification. Local cross-section contraction results in local flow velocity increase. Such contraction is commonly used to increase the flow velocity in the point of flow transducer location. But tapered duct downstream the bluff body improves the generated vortices due to the flow velocity increase. As the result, the flowmeter lower range limitation is shifted towards lower flow velocities. The fact that the contraction appears only in limited zone close to the bluff body results in the meter pressure loss limitation.

4. Numerical modelling of the vortex development in the tapered duct

The numerical modelling of the vortex development in the tapered duct also bases on the division of the flow area downstream bluff body into three zones:

- intensive development zone,
- stabilization zone,
- vortices decay zone.

The modified flow duct is presented in Fig.2.

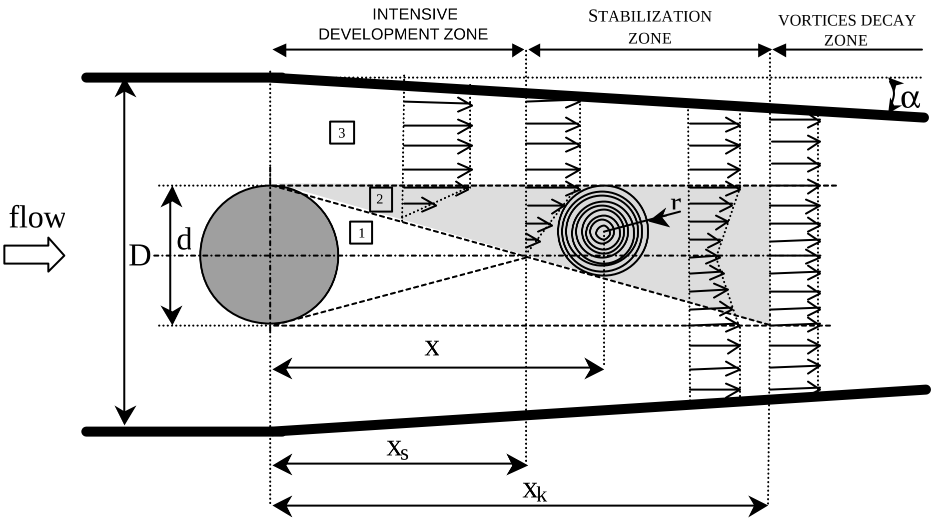

Fig. 2. Vortex development behind bluff body in tapered duct
(1 - stagnation region, 2 - region of steady velocity profile, 3 - region of vortices development)

Analysing the fluid velocity distribution in the area downstream the bluff body, it can be noticed, that increase of the fluid velocity forcing the vortex depends on the tapered angle α.

In **the intensive development zone,** the velocity "driving" the added layer depends on the contraction angle α and is greater than in the duct of steady cross-section:

$$\mathbf{v_{pc}} = \frac{\mathbf{v}}{2} \cdot \frac{\mathbf{D}}{\mathbf{D} - \mathbf{d} + \mathbf{x} \cdot \left(\frac{\mathbf{d}}{2 \cdot \mathbf{x_s}} - 2 \cdot \mathbf{tg}\,\alpha \right)} \qquad \mathbf{(6)}$$

and rotation of the generated layer is expressed by eq.:

$$\omega = \frac{\mathbf{v} \cdot \mathbf{x_s}}{\pi \cdot \mathbf{d} \cdot \mathbf{x}} \cdot \frac{\mathbf{D}}{\mathbf{D} - \mathbf{d} + \mathbf{x} \cdot \left(\frac{\mathbf{d}}{2 \cdot \mathbf{x_s}} - 2 \cdot \mathbf{tg}\,\alpha\right)} \tag{7}$$

Although in **the stabilization zone**, forcing of the consecutively added layers becomes considerably weaker along with the distance **x** than in the intensive development zone, but due to the duct tapering the velocity forced the added layers reaches higher values (in comparison with the steady cross-section duct):

$$\mathbf{v_{pc}} = \mathbf{v} \cdot \left(1 - \frac{\mathbf{x}}{2 \cdot \mathbf{x_s}}\right) \cdot \frac{2 \cdot \mathbf{D} \cdot (\mathbf{x_k} - \mathbf{x}) + 4 \cdot \mathbf{x} \cdot (\mathbf{x} - \mathbf{x_s}) \cdot \mathbf{tg}\,\alpha}{(\mathbf{x_k} - \mathbf{x_s}) \cdot (2 \cdot \mathbf{D} - \mathbf{d} - 4 \cdot \mathbf{x} \cdot \mathbf{tg}\,\alpha)} \tag{8}$$

rotation of the generated layer is expressed by:

$$\omega = \frac{2 \cdot \mathbf{v} \cdot \mathbf{x_s}}{\pi \cdot \mathbf{d} \cdot \mathbf{x}} \cdot \left(1 - \frac{\mathbf{x}}{2 \cdot \mathbf{x_s}}\right) \cdot \frac{2 \cdot \mathbf{D} \cdot (\mathbf{x_k} - \mathbf{x}) + 4 \cdot \mathbf{x} \cdot (\mathbf{x} - \mathbf{x_s}) \cdot \mathbf{tg}\,\alpha}{(\mathbf{x_k} - \mathbf{x_s}) \cdot (2 \cdot \mathbf{D} - \mathbf{d} - 4 \cdot \mathbf{x} \cdot \mathbf{tg}\,\alpha)} \tag{9}$$

In **vortices decay zone**, similarly like in the model with steady cross-section, although new layers are added to the vortex, they are not forced by the stream.

5. Energy relationships and viscosity impact

From the practical point of view, the most significant parameter of the vortex is its rotation energy. The electrical signal obtained from the sensor (detector of vortices) directly depends on the rotation energy. Hence the necessity of the energy calculation. It is based on the fundamental relationship:

$$\mathbf{E_{rot}} = \frac{1}{2} \cdot \mathbf{J} \cdot \omega^2 \tag{10}$$

Because of the fact, that in the model the vortex consists of certain number of coaxial layers, the total rotation energy of the vortex is a sum of energies calculated separately for each layer:

$$\mathbf{E_{tot}} = \sum_{k=1}^{n} \mathbf{E_{rot(k)}} \tag{11}$$

The viscosity impact on the vortex rotation energy origins in the difference of the adjacent layers rotation. The difference results from the fact, that each layer of the vortex gets the rotation respectively to the point of its origin. Because of the fact, that the model of the vortex development assumes continuous wiring on the subsequent layers, the current energy of the vortex is equal the sum of energies of the layers. Simultaneously, due to the fluid viscosity, the adjacent layers interact each other diminishing the local velocity gradient. The rotation of the adjacent layers aims at becoming even. In the model the conservation of momentum principle has been applied. The energy distribution in the vortex is modified as well as the energy losses are observed. Hence the total rotation energy decrease, particularly visible in the vortices decay zone.

6. Comparison of vortex development in the model with steady cross-section and with tapered duct

On the basis of created models, the vortex development in both: the duct of steady cross-section and in the tapered duct may be compared. Fluid velocity “driving” the vortex vs. distance from its origin for both cases is shown in Fig.3.

In the case of the duct with steady cross-section the velocity gradually decreases, especially in the stabilization zone. Hence diminishing of the energy of the consecutively added layers to the vortex. As the result, the vortices energy growth is limited.

Due to the duct contraction, the local velocity “driving” the vortex considerably increases in the intensive development zone. Also in the stabilization zone the obtained velocities reach higher values comparing with the steady cross-section duct.

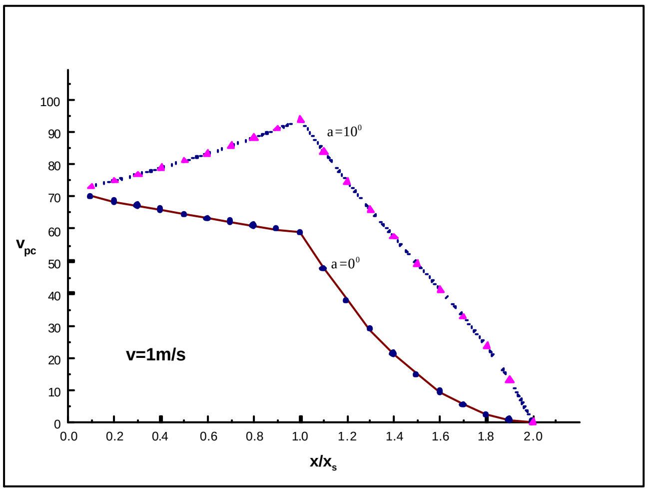

Fig.3. Velocity “driving” the vortex vs. distance from bluff body axis for duct of steady cross-section and for tapered duct

It is worth to remark that already with the contraction angle $a = 4.5^0$ the constant velocity in the intensive development zone is kept.

Rotation energy of the vortex (being a sum of energies of all layers) should be treated as fundamental measure of the applied phenomenon quality. Rotation energy of the vortex as a function of its current position is presented in Fig.4.

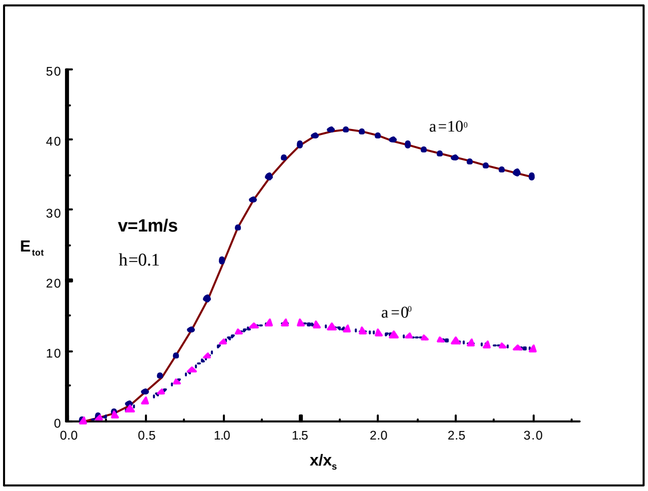

Fig.4. Rotation energy vs. distance from bluff body axis for duct of steady cross-section and for tapered duct

As it is easy to notice, considerable increase of the rotation energy due to the duct contraction is observed. For the contraction angle $a = 10^0$ the maximal rotation energy is 3 times greater than in the case of steady cross-section duct. It is also worth to remark that the maximum energy occurs for grater distance from the vortex origin (on the bluff body surface). It means that the process of the vortex decay becomes later in fact. It should be underlined, that it is profitable from the point of view of the flow meter designing.

7. Hot-wire anemometer tests

Laboratory investigations using the hot-wire anemometer system application have been carried out on the specialized measuring stand for gas flowmeters calibration [2]. Especially designed module enabled the hot-wire 2D probe displacement along with x,y co-ordinates. Flow velocity distribution in the plane perpendicular to the bluff body axis has been determined. On the basis of the signals obtained from the probes, two axial components of the velocity and their turbulences have been calculated.

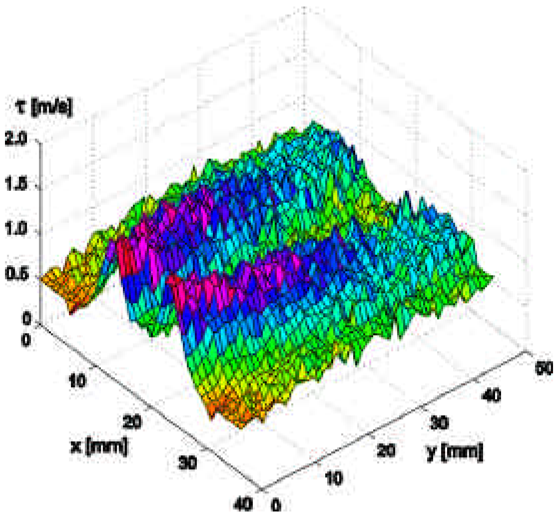

Fig.5. Lengthways turbulence distribution for steady cross-section duct

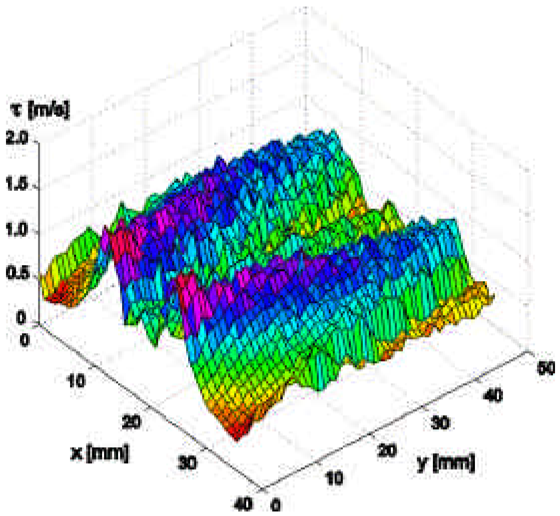

Fig.6. Lengthways turbulence distribution for tapered duct

Lengthways turbulence distributions for both cases of the duct: with steady cross-section and tapered one are shown in Fig.5 and Fig.6. Analysing obtained pictures it is visible considerable vortex time-life increase in the case of the tapered duct. Although in the area close the bluff body the graphs are similar, the differences are significant for the greater distances from the bluff body (y>35 mm). Obviously, enlargement of the area of stable vortices is profitable from the point of view of the meter designing.

It is also worth to remark, that laboratory investigations did not confirm the considerable – resulted from the numerical modelling – increase of the vortex rotation energy. This problem will be particularly taken into consideration in future investigations.

8. Conclusions

New configuration of the vortex meter has been proposed. Due to the duct contraction, the considerable improvement of the measuring signal quality is expected. On the basis of numerical simulation it may be concluded, that the duct contraction causes essential increase of the velocity "driving" the vortex. It results in increase of the vortex rotation energy as well. Very interesting is also the fact, that due to the duct contraction, the vortex time-life increase has been attained. It was clearly confirmed by the laboratory tests carried out by hot-wire anemometer system.

It is necessary to underline, that the extension of the duct contraction is limited. Too great contraction can cause the vortex quality deterioration as well as pressure losses increase.

References: [1] Pankanin G.L., Berlinski J., Chmielewski R.: *Numerical Modelling of Karman Vortex Street* - Proc. of Fifth Triennal International Symposium on Fluid Control, Measurement and Visualization FLUCOME'97, Hayama 97, Japan, pp. 761-765

[2] Berlinski J., Chmielewski R., Pankanin G.L.: *Vortex Flow Field Investigations with Application of Hot-Wire Anemometer* - Proc. of International Conference of Flow Measurement FLOMEKO 2000, Salvador, 6-10 May 2000, Brazil, CD-Rom proceeding